Chemistry
A European
Journal

Chemistry Europe
European Chemical Societies Publishing

Accepted Article

Title: Synthesis of Three-Dimensional (3D) (Di)azatricyclododecene Scaffold and its Application to Peptidomimetics

Authors: Kohei Umedera, Taiki Morita, Atsushi Yoshimori, Kentaro Yamada, Katoh Akira, Hiroyuki Kouji, and Hiroyuki Nakamura

To be cited as: *Chem. Eur. J.* 10.1002/chem.202101440

Link to VoR: https://doi.org/10.1002/chem.202101440

WILEY-VCH

10.1002/chem.202101440

WILEY-VCH

RESEARCH ARTICLE

Synthesis of Three-Dimensional (3D) (Di)azatricyclododecene Scaffold and its Application to Peptidomimetics

Kohei Umedera,[a] Taiki Morita,[a,b] Atsushi Yoshimori,[c] Kentaro Yamada,[d,e] Akira, Katoh, [e,f] Hiroyuki Kouji,[e,f] and Hiroyuki Nakamura*[a,b]

[a] K. Umedera, Dr. T. Morita, Prof. Dr. H. Nakamura
School of Life Science and Technology
Tokyo Institute of Technology
Yokohama, 226-8503, Japan
[b] Dr. T. Morita, Prof. Dr. H. Nakamura
Laboratory for Chemistry and Life Science, Institute of Innovative Research
Tokyo Institute of Technology
Yokohama, 226-8503, Japan
E-mail: hiro@res.titech.ac.jp
[c] Dr. A. Yoshimori
Institute for Theoretical Medicine, Inc.
26-1, Muraoka-Higashi 2-chome, Fujisawa, 251-0012, Japan
[d] Dr. K. Yamada
Faculty of Agriculture Department of Veterinary Sciences
University of Miyazaki
Miyazaki, 889-2192, Japan
[e] Dr. H. Kouji, Dr. K. Yamada, Dr. A. Kato
Faculty of Medicine
Oita University
1-1, Idaigaoka, Hasama-machi, Yufu-city, Oita, 879-5593, Japan
[f] Dr. H. Kouji, Dr. A. Katoh
Oita University Institute of Advanced Medcine, Inc.
17-20, Higashi kasuga-machi, Oita-city, Oita 870-0037, Japan

Supporting information for this article is provided via a link at the end of the document.((Please delete this text if not appropriate))

Abstract: A novel sp^3 carbon-rich tricyclic 3D scaffold-based peptide mimetic compound library was constructed to target protein-protein interactions. Tricyclic framework **6** was synthesized from 9-azabicyclo[3,3,1]nonan-3-one **9** via a gold (I)-catalyzed Conia-ene reaction. The electron-donating group on the pendant alkyne of cyclization precursor **11b-e** was the key to forming 6-*endo-dig* cyclized product **6** with complete regioselectivity. Using the synthetic strategy for regioselective construction of bridged tricyclic framework **6**, a diazatricyclododecene 3D-scaffold **7a**, which enables the introduction of substituents into the scaffold to mimic amino acid side chains, was designed and synthesized. The peptide mimetics **20a-h** were synthesized via step-by-step installation of three substituents on diazatricyclododecene scaffold **7a**. Compounds **20a-h** were synthesized as α-helix peptide mimics of hydrophobic ZZxxZ and ZxxZZ sequences (Z = Leu or Phe) and subjected to cell-based assays: antiproliferative activity, HIF-1 transcriptional activity which is considered to affect cancer malignancy, and antiviral activity against rabies virus. Compound **20a** showed the strongest inhibitory activity of HIF-1 transcriptional activity (IC_{50} = 4.1 ± 0.8 μM), whereas compounds **20a-g** showed antiviral activity with IC_{50} values of 4.2-12.4 μM, suggesting that the 3D-scaffold **7a** has potential as a versatile peptide mimic skeleton.

Introduction

Molecular shape is one of the most fundamental factors in protein molecular recognition. Therefore, compound libraries with structural diversity are highly needed for targeting a wide variety of proteins. However, the biased use of aromatic rings in the synthesis of drugs or their candidates tends to make the molecule sp^2 carbon-rich and planar.[1,2] Conventional small molecule libraries have been constructed by sp^2 carbon-rich planar molecules and mainly targeted enzymes. In order to discover small molecule modulators for promising biological targets such as protein-protein interactions (PPIs),[3] there is a growing interest in employing sp^3 carbon-rich 3D scaffolds to access unexplored chemical spaces. Synthetic strategies to construct structurally diverse compound collections, such as diversity-oriented synthesis[4] and biology-oriented synthesis,[5] have provided compounds with unique biological activities, including PPI inhibition[6] and protein-DNA interaction inhibition.[7] Psuedo-natural product design,[8] which combines two different natural product scaffolds in an sp^3 carbon-rich manner, has provided an autophagy inhibitor.[9] Compound libraries based on 3D natural product scaffolds have shown a wide range of biological activities.[10] These observations strongly support the high utility of 3D scaffolds in drug discovery.

The FDA has recently approved Venetoclax (ABT-199) as a first-in-class small molecule-based PPI inhibitor targeting the Bcl-2/Bax interaction.[11] It was rationally designed based on the structure of hydrophobic groove binding site in Bcl-x_L.[12] Therefore, the design of peptidomimetics targeting PPIs has been recognized as a promising strategy for the rational development of small molecule-based inhibitors.[13] The first small molecule-based α-helix mimetic was reported by Rees et al.[14] They utilized 1,6-disubstituted indane as a template for two adjacent amino acid chains of a protein α-helix motif.

10.1002/chem.202101440

Pioneering work was accomplished by Hamilton et al., who reported that an α-helix mimetic of the α-helical domain of smooth muscle myosin light-chain kinase (smMLCK) based on the terphenyl scaffold **1** was able to inhibit PPI between calmodulin and smMLCK (Figure 1a).[15] Inspired by their simple and rational molecular design concept of peptidomimetics based on aromatic scaffolds with peptide side-chains, a variety of scaffolds, such as benzamide **2**,[16] pyrdazine **3**,[17] and pyrroloprimidine **4**,[18] have been developed to mimic the α-helix structure. However, these scaffolds are primarily dependent on aromatic compounds, and the biased use of aromatic rings for designing peptidomimetics limits their therapeutic targets as other conventional drugs. Peptides are chirality-rich and structurally complex; therefore, sp^3 carbon-rich scaffolds can be considered as suitable scaffolds for designing small molecule-based peptide mimetics. Arora et al. desgined an α-helix mimetic based on a non-aromatic oligooxopiperazine scaffold **5.**[19] The peptidomimetic was found to inhibit PPI between hypoxia-inducible factor (HIF)-1α and p300, a promising target for cancer therapy.[20] These results suggest the importance of compound complexity in designing peptidomimetics.

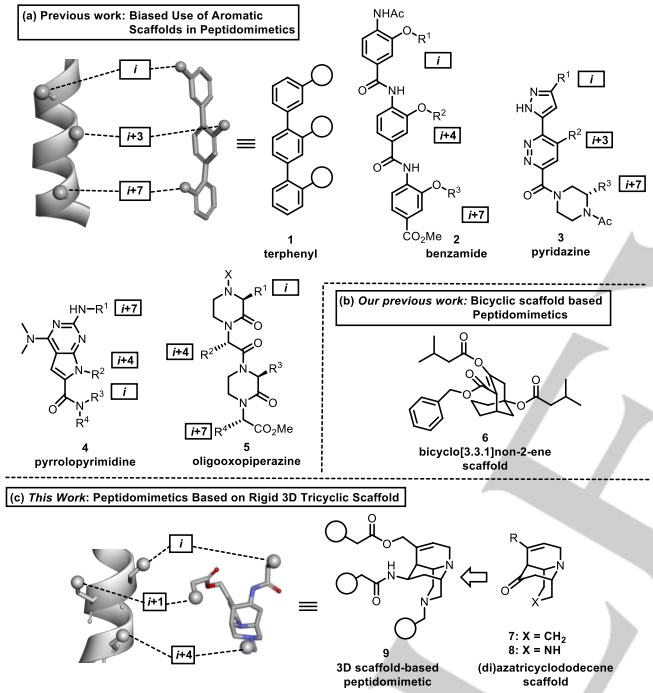

Figure 1. Structure of small molecule-based peptidomimetics: (a) structures of previously designed α-helix mimetics, (b) bicyclo[3.3.1]non-2-ene scaffold (**6**), (c) (di)azabicyclo scaffolds (**6** and **7**) and 3D scaffold-based peptidomimetic (**8**).

We previously reported α-helix mimetics based on bicyclo[3,3,1]non-2-ene as a 3D scaffold **6** (Figure 1b).[21] In contrast to aromatic rings, the bridged bicyclic scaffold was rich in sp^3 carbons and highly three-dimensional. The peptide mimetics were designed to reproduce the three leucine residues (Leu818, Leu819, and Leu822) of the C-terminal helix (helix 3) of HIF-1α. Although the mechanism of action has not been clarified, the molecules can inhibit HIF transcriptional activity. The design of peptidomimetics based on rigid 3D scaffolds would be an efficient strategy for exploring the chemical space and discovering compounds with beneficial biological activities. In addition to HIF transcriptional activity, PPI via the α-helix plays a pivotal role replicating rabies virus. Rabies is an infectious disease caused by the rabies virus and can be treated with a post-exposure vaccine if the symptoms have not yet appeared. However, the fatality rate is approximately 100% upon the appearance of the symptoms, and no therapeutic drugs have been reported.[22] Rabies virus RNA is known to be condensed by nucleoprotein oligomers into helical nucleocapsids, and this nucleoprotein-RNA complex constitutes an essential template for replication by RNA polymerase. The C-terminal α-helix 16 of the rabies nucleoprotein, containing the FxxFL sequence (Phe438, Phe441, and Leu442), contributes to robust oligomer formation.[23] We also predicted that the FxxFL sequence of the rabies virus nucleoprotein could be mimicked using a similar strategy to design a peptidomimetic of the LLxxL sequence of HIF-1α.

Herein we report the development of azatricyclododecene **7** and diaztricyclododecene **8** as novel 3D scaffolds (Figure 1c). Tricyclic framwork of **7** and **8** was insipired by adding another ring to bridged bicyclic structure **6**, which was employed in our previous work[21]. Peptidomimetic **9** was designed based on scaffold **8**, and its compound libraries were constructed. The newly designed peptidomimetics characterized by high threedimensionality and precise arrangement of substitutents mimicking peptide side-chains could expand the chemical space and discover bioactive compounds. Cell-based assays were conducted to evaluate the antiproliferative activity, inhibitory effect on HIF transcriptional activity, and anti-rabies virus activity of the synthesized compounds.

Results and Discussion

A synthetic strategy for the designed bridged tricyclic is shown in Scheme 1a. We envisioned that the the desired tricyclic framework **7** could be constructed from amine **10** *via* gold (I)-catalyzed Conie-ene reaction[24]. Tertiary amine **10** was expected to be easily obtained by propalgylation of 9-azabicyclo[3,3,1]nonan-3-one (**11**) which is known to be readily prepared by Mannich cyclization.[25,26]

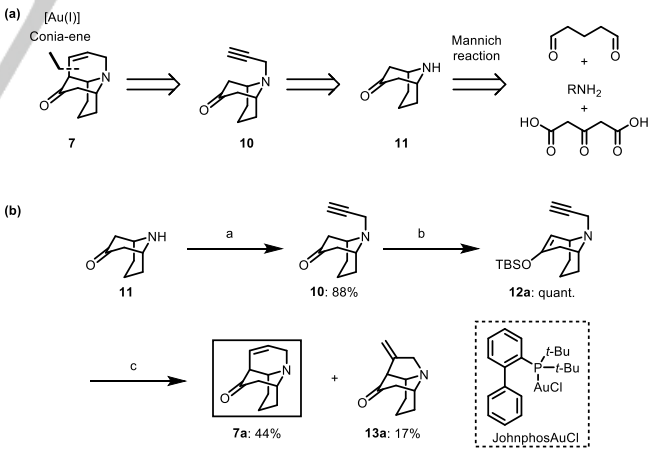

Scheme 1. (a) Retorosynthetic analysis of azatricyclododecen **7**, (b) Synthesis of azatricyclododecene **7a**. Reaction conditions: a) propargyl bromide, K_2CO_3, MeCN, rt, 2.5 h; b) TBSOTf, 2,6-lutidine, CH_2Cl_2, -78 ºC to 0 ºC, 40 min; c) JohnPhosAuCl (10 mol%), AgOTf (15 mol%), toluene/MeOH = 10:1, 40 ºC, 24 h. TBS = *tert*-butyldimethylsilyl, Tf = trifluoromethanesulfonyl, Johnphos = (2-biphenyl)di-*t*-butylphosphine

Treating 9-azabicyclo[3,3,1]nonan-3-one (**10**), which was synthesized *via* three component coupling of 1,3-acetonedicarboxylic acid, glutaric dialdehyde, and ammonia,[25,26] with propargyl bromide afforded the corresponding tertiary amine **10** in 88% yield. By treating

10.1002/chem.202101440

ketone **10** with TBSOTf and 2,6-lutidine, silyl enol ether **12a** was obtained as a precursor for the bridged tricyclic skeleton in quantitative yield. Thereafter, **12a** was subjected to gold (I)-catalyzed Conia-ene reaction.[24] The desired 6-*endo*-dig cyclization proceeded in the presence of a catalytic amount of JohnphosAuCl and AgOTf to provide azatricyclododecene **7a** in 44% yield with the generation of 5-*exo-dig* cyclized product **13a** in 17% yield.

To improve the yield of 6-*endo*-cyclized product **7** in a highly regioselective manner, we investigated the gold (I)-catalyzed cyclization of **12**. Screening of ligands and silver salts did not significantly improve regioselectivity (see Table S1). Thereafter, the effects of substituent R on the pendant alkyne were examined (Table 1). It has been reported that the regioselectivity of the gold(I)-catalyzed intramolecular cyclization depends on the electronic effect of the substituents.[27] Therefore, we tested various types of precursors **12a-i** with different substituents on the alkyne moiety. When substrate **12b**, which has 4-methoxyphenyl group on alkyne was treated with cationic gold catalyst, the desired 6-*endo-dig* cyclized product **7b** was obtained in good yield (75%) with complete regioselectivity (entry 2). Similarly, the use of alkyl groups, such as the siloxymethyl group (entry 3), phthalimidylmethyl group (entry 4), and methyl group (entry 5), led to the selective formation of six-membered rings to provide the corresponding products in good yields (**7c**: 67%, **7d**: 55%, **7e**: 66%). In contrast, electron-withdrawing groups such as the trifluoromethyl group (entry 6), ethoxycarbonyl group (entry 7), and amide group (entry 8) selectively induced 5-*exo-dig* cyclization to give products **13f-h** as a single diastereomer. Iodoalkyne **12i** was not converted into the corresponding cyclized products **7i** and **13i**; however, it resulted in a complex mixture (entry 9). These results suggest that electron-donating groups on the alkyne prefer the 6-*endo* cyclization mode.

Table 1. Investigation of regioselectivity of the gold(I)-catalyzed cyclization[a]

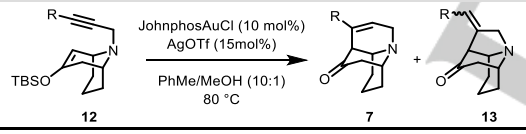

entry	substrate	R	Products	Yield[b] (%) of **7**/**13**
1[c]	**12a**	H	**7a**/**13a**	44/17
2[c]	**12b**	4-MeOC$_6$H$_5$	**7b**/**13b**	75[d]/0
3[c]	**12c**	TBSOCH$_2$	**7c**/**13c**	67[d]/0
4	**12d**	PhthNCH$_2$	**7d**/**13d**	55[d]/0
5	**12e**	Me	**7e**/**13e**	66[d]/0
6	**12f**	F$_3$C	**7f**/**13f**	0/25[d] (45)[f]
7	**12g**	EtOCO	**7g**/**13g**	0/50[d]
8	**12h**	*n*-BuNHCO	**7h**/**13h**	0/36[d]
9	**12i**	I	**7i**/**13i**	0/0[e]

[a] Standard conditions: JohnPhosAuCl (10 mol%), AgOTf (15 mol%), toluene/MeOH = 10:1, 80 °C, 13.5–24 h. [b] Isolated yield. [c] The reaction was performed at 40 °C. [d] Single diastereomer. [e] Complex mixture. [f] Recovery of **13g** in parentheses. Ph = phenyl, TMS = trimethylsilyl, PhthNCH$_2$ = phthalimidyl methyl, Et = ethyl, Bu = butyl.

With a successful construction of bridged tricyclic skeleton, we turned our attention to the synthesis of diazatricylododecene **8** (Scheme 2), which enables the introduction of substituents into the scaffold to mimic amino acid side chains as shown in Figure 1b. To embed one more nitrogen atom into the tricyclic framework **7**, imide **14** was selected as the starting material. Reduction of imide **14** with LiAlH$_4$, followed by removal of the benzyl group, and subsequent protection of the resulting secondary amine with the Cbz group afforded diol **15** in 43% yield in three steps. The oxidative cleavage of *trans*-configured diol **15** using NaIO$_4$ afforded dialdehyde **16**.[28] After *N*-propargylation using propargyl iodide **18**,[29] the corresponding tertiary amine **19** was isolated in 33% yield in three steps. Cyclization precursor **20** with a siloxymethyl group on the alkyne was prepared quantitatively by transforming ketone **19** into silyl enol ether. Thereafter, the substrate **20** was subjected to the gold(I)-catalyzed Conia-ene reaction. As a result, an alkyl group on the alkyne expectedly enabled the selective formation of the 6-*endo-dig* cyclized product. The subsequent removal of the Cbz group produced the desired diazatricyclododecene **8a** in 79% yield in two steps.

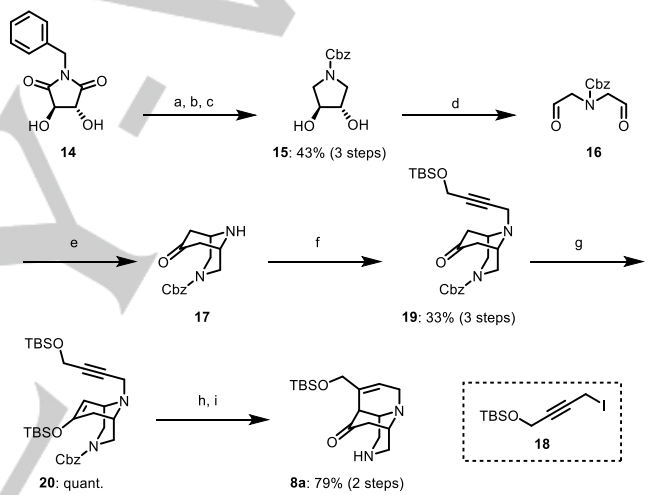

Scheme 2. Synthesis of diazatricyclododecene **8a**. Reaction conditions: a) LiAlH$_4$, THF, 90 °C, 3.5 h; b) Pd/C, H$_2$, MeOH, 50 °C, 4 h; c) CbzOSu, Na$_2$CO$_3$, H$_2$O, 1,4-dioxane, 0 °C, 2.5 h; d) NaIO$_4$, H$_2$O, Et$_2$O, rt, 19 h; e) 1,3-acetonedicarboxylic acid, NH$_3$, H$_2$O, 0 °C to rt, 46 h; f) **19**, K$_2$CO$_3$, MeCN, rt, 7.5 h; g) TBSOTf, Et$_3$N, CH$_2$Cl$_2$, −78 °C to 0 ºC, 10 min; h) JohnPhosAuCl, AgOTf, toluene/MeOH = 10:1, 40 °C 1.5 h; i) Rh/Al$_2$O$_3$, H$_2$, MeOH, 50 °C, 11 h. Cbz = Carbobenzyloxy, OSu = oxysuccinimide.

With a novel diazatricyclo scaffold **8a**, we designed peptidomimetics by introducing three substituents, mimicking the leucine residue (R = *i*-Bu) or phenylalanine residue (R = Bn), on the tricyclic scaffold (Figure 2a). The validity of the designed molecule **21** as a mimetic of helix 3 was evaluated by pharmacophore modeling using LigandScout 4.4.[30] Conformers of the designed molecules were generated using 'iCon Fast' option and screened to assess whether the generated structures could achieve three hydrophobic features derived from the target peptides. Compound **21a** was found to reproduce the spatial orientation of the LLxxL sequence in HIF-1α (Figure 2b). Similarly, compound **21b** mimicked the spatial arrangement of the FxxFL sequence in the nucleoprotein of the rabies virus (Figure 2c). These results suggest that the designed skeletal molecule **21** may serve as a versatile peptide mimic.

10.1002/chem.202101440

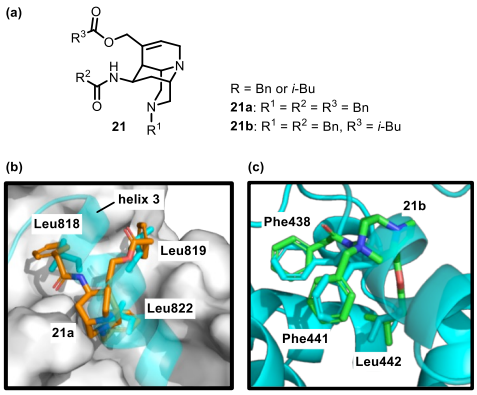

Figure 2. Design of peptidomimetics based on diazatricyclododecene scaffold. (a) Structure of designed peptidomimetic **21**, (b) Superimposition of **21a** and helix 3 of HIF-1α (PDB ID: 1L8C), (c) Superimposition of **21b** and rabies virus nucleoprotein (PDB ID: 2GTT).

Due to its the potential as a peptidomimetic, a compound library of mimetics **21** was constructed via step-by-step installation of three substituents on the diazatricyclododecene scaffold **8a** (Scheme 3A). For diazatricyclododecene **8a**, the first substituents were introduced to secondary amine moiety by reductive amination to afford tertiary amines **22a** and **22b**. Thereafter, azides **23a** and **23b** were prepared through carbonyl reduction with $LiAlH_4$, mesylation of the resulting alcohol, and azidation using NaN_3. Subsequent Staudinger reduction furnished amines **24a** and **24b**. The second substituents were introduced by condensation with the corresponding carboxylic acids to afford amides **25a-d**. The structure of amide **25b** was unambiguously determined by X-ray crystallographic analysis, and the stereoselective installation of an azide group was confirmed. Finally, the third substituent was introduced through a sequence of TBS deprotection and esterification to provide the desired peptidomimetics **21a-h**.

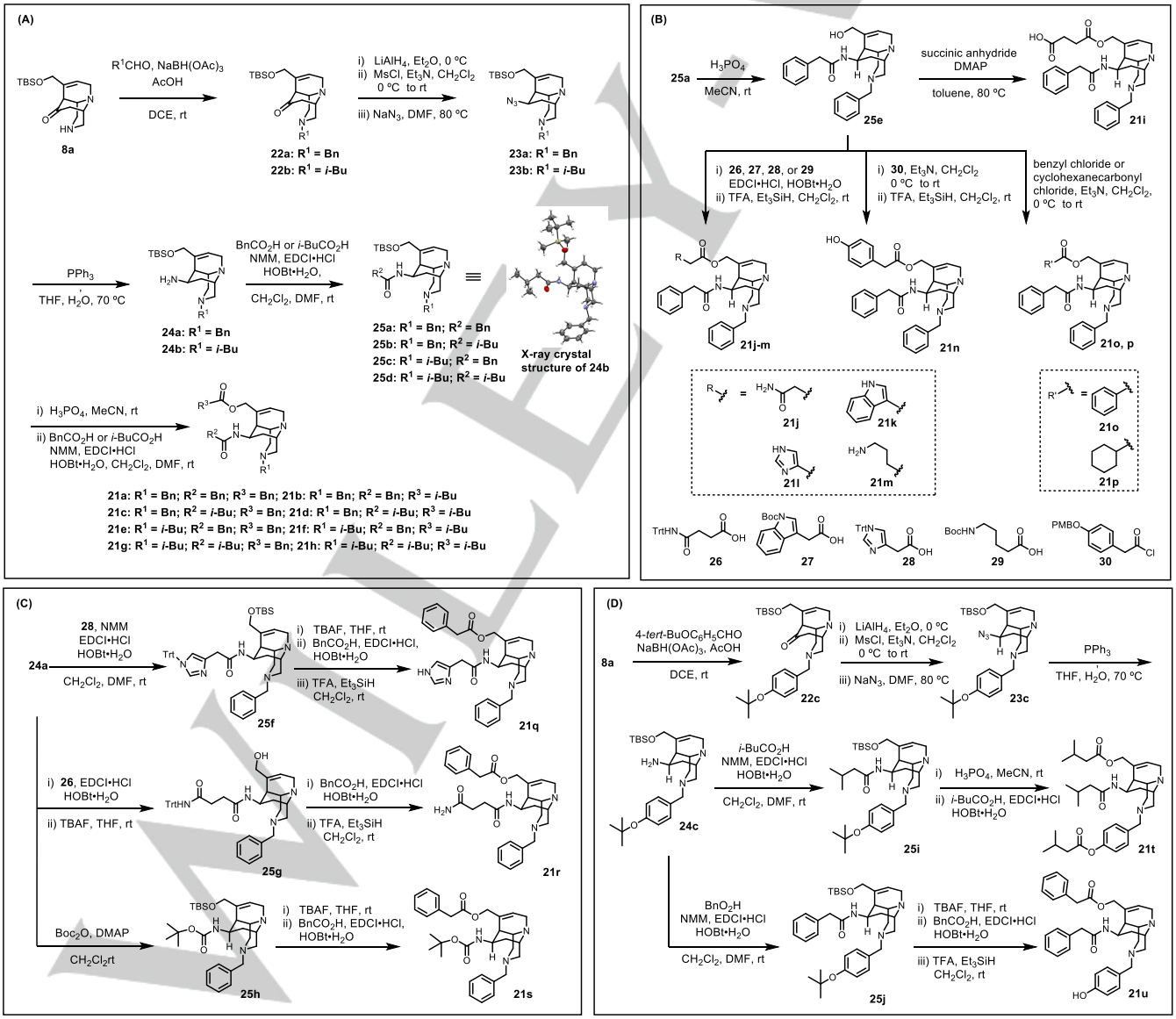

10.1002/chem.202101440

Scheme 3. Construction of compound library. (A) Synthesis of helix 3 mimetics. (B) Derivatization of R^3 group. (C) Derivatization of R^2 group. (D) Derivatization of R^1 group.. Trt = trityl; Boc = *tert*-butoxycarbonyl; PMB = *p*-methoxybenzyl, Bn = benzyl, Ac = acetyl, DCE = 1,2-dichloroethane, Ms = methanesulfonyl, NMM = *N*-methylmorpholine, EDCI = 1-ethyl-3-(3-dimethylaminopropyl)carbodiimide, HOBt = 1-hydroxybenzotriazole, DMF = *N*,*N*-dimethylformamide, TFA = trifluoroacetic acid, TBAF = tetrabutylammonium fluoride, DMAP = 4-dimethylaminopyridine.

For drug development, the modular synthesis of derivatives with various substituents on a scaffold is highly required. Therefore, the compound library was further expanded by assembling various functional groups rather than isobutyl or benzyl group. As a result, the derivatization of R^3 was first demonstrated as shown in Scheme 3B. After TBS deprotection of intermediate **25a**, eight more substituents were introduced as R^3 via esterification. Diverse functional groups, including carboxylic acid, amide, heterocycles, amine, and phenol were tolerated, and **21i-p** were obtained. To diversify the R^2 group (Scheme 3C), amine **24a** was coupled with carboxylic acids **28** and **26** to afford **25f** and **25g**, respectively. It was also possible to introduce the Boc group into the R^2 group, and the corresponding carbamate **25h** was obtained. Following the same protocols as in Scheme 3A, trisubstituted **21q-s** with the Bn group as R^3 were provided. As a variation of the R^1 group, a phenoxy group was introduced (Scheme 3D). Conjugation of diazatricyclododecene **8a** and 4-*tert*-butoxybenzaldehyde via reductive amination afforded tertiary amine **22c**, which was converted to primary amine **24c** through **23c** following the established procedure shown in Scheme 3A. After introducing isobutyl group to afford **25i**, acidic removal of both TBS and *tert*-Bu groups, followed by condensation with isovaleric acid afforded diester **21t**, was performed. Instead of diester, the treatment of amide **25j** with TBAF, followed by a sequence of esterification and acidic removal of the *tert*-Bu group presented phenol **21u**.

Molecular shape of synthesized compounds were compared with approved drugs in DrugBank database (v.5.1.7) using principle moment of inertia (PMI)[31] based on their lowest-energy conformations generated by 'iCon Fast' option of LigandAcout4.4. (Figure 3). While approved drugs were congested along the rod or disc-like axis, our synthesized compounds were widely distributed around the right center field of the triangle. The analysis suggests that compared to conventional drugs, our compounds are more three-dimensional, which has been a highly demanded feature for a bioactive compound library.

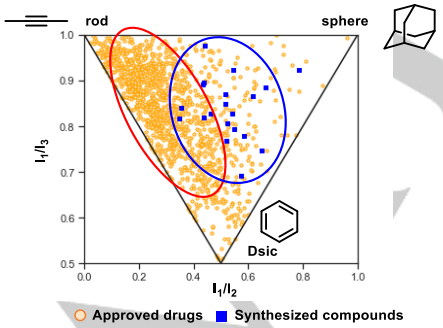

Figure 3. PMI analysis of synthesized compounds and approved drugs in DrugBank database.

We selected compounds **20a-h** as mimics of hydrophobic ZZxxZ and ZxxZZ sequences (Z = Leu or Phe), which exist in helix 3 and rabies nucleoprotein, respectively, and performed cell-based assays: anti-proliferative activity, HIF-1 transcriptional activity, and antiviral activity (Table 2). Prior to the following luciferase reporter gene assay, the MTT assay was conducted to evaluate the antiproliferative activity of helix 3 mimetics **21a-h** against human epithelioid cervical carcinoma HeLa cells and Neuro 2a (N2a) cells. All compounds inhibited the growth of N2a cells more significantly compared to HeLa cells (entries 3-10). Compound **21a** was the most potent to inhibit the growth of both HeLa and N2a cells with IC_{50} values of 10.3 ± 0.8 μM and 2.1 ± 0.6 μM, respectively (entry 3).

To verify the α-helix mimic strategy, the inhibitory effect on HIF transcriptional activity was evaluated using a cell-based reporter gene assay. HeLa cells transfected with a hypoxic response element (HRE)-dependent luciferase reporter gene were incubated under hypoxic conditions in the presence of compounds, and their IC_{50} values were determined (Table 2). YC-1,[32] an inhibitor of HIF-1 activity, was used as a positive control. Among the compounds synthesized, compound **21a** (entry 1) showed the strongest inhibitory activity (IC_{50} = 4.1 ± 0.8 μM), with a level similar to YC-1 (entry 9). However, **21a** also inhibited the growth of HeLa cells with IC_{50} value of 10.3 ± 0.8 μM. Therefore, the cytotoxicity of **21a** may affect the inhibition of HIF transcriptional activity. Among compounds with low cytotoxicity against HeLa cells (MTT IC_{50} > 30 μM), compound **21c** (entry 5) was the most potent inhibitor of HIF transcriptional activity (IC_{50} = 9.1 ± 1.8 μM).

Antirabies viral activity was also examined. Rabies virus RNA fused with Gaussia luciferase reporter was incubated with N2a cells in the presence of compounds up to 18 μM. IC_{50} values were determined by measuring the luciferase activity in the cell supernatant secreted extracellularly. Favipiravir (T-705),[33] an antiviral agent, was used as a positive control. Compounds **21a-g** were found to exhibit antiviral activity with IC_{50} values of 4.2–12.4 μM (entries 3–9), suggesting that these compounds are more potent than the known antiviral T-705. Since the antiproliferative inhibitory activities of **21a-g** against N2a cells are comparable to the inhibition of anti-rabies viral activity, the observed antiviral activity may be attributed to cytotoxicity against host cells. However, there was no correlation between the IC_{50} values of the MTT assay against N2a cells and the luciferase reporter gene assay for antiviral activity. Therefore, at least part of the inhibitory effect could be attributed to the antiviral effect, indicating the potential of peptidomimetics to be developed as antiviral drugs.

Table 2. Evaluation of bioactivity of helix 3 mimetics **21a-h**

entry	compound	Antiproliferative activity: IC_{50} (μM)[a]		Inhibition of HIF transcriptional activity: IC_{50} (μM)[a]	Anti-rabies viral activity: IC_{50} (μM)[a]
		HeLa	N2a		
1	**21a**	10.3 ± 0.8	2.1 ± 0.6	4.1 ± 0.8	11.0 ± 3.6
2	**21b**	15.9 ± 2.6	3.4 ± 1.0	11.0 ± 0.1	4.2 ± 1.2
3	**21c**	> 30	9.2 ± 2.0	9.1 ± 1.8	12.4 ± 4.3
4	**21d**	> 30	5.6 ± 0.4	21.2 ± 2.2	9.7 ± 3.0

5	**21e**	16.9 ± 4.3	3.9 ± 1.2	12.5 ± 2.7	11.6 ± 0.9
6	**21f**	25.7 ± 0.4	4.8 ± 0.1	18.9 ± 6.0	12.1 ± 0.5
7	**21g**	> 30	11.8 ± 1.6	11.7 ± 4.2	8.3 ± 3.3
8	**21h**	> 30	17.8 ± 1.7	> 30	> 18
9	YC-1	-[b]	-[b]	2.9 ± 1.3	-[b]
10	T-705	-[b]	-[b]	-[b]	37.7

[a] Indicated values are mean ± SD of single experiment conducted in triplicate. [b] Not determined.

Conclusion

We have developed a novel 3D-shaped diazatricyclododecene scaffold featuring a constrained bridging tricyclic core. Synthetic studies on the gold(I)-catalyzed cyclization of monoaza substrate **12** revealed that the electron-donating group on the pendant alkyne is the key to the formation of 6-*endo-dig* cyclized product **7** with complete regioselectivity. The established synthetic strategy allowed the generation of the diazatricyclododecne scaffold **8a**, and the stepwise assembly of the three substituents resulted in the generation of diversely functionalized compounds **21a-u**. Biological assays of designed mimics of helix-3 of HIF-1α and the α-helix 16 of rabies virus nucleoprotein indicated that some helix-mimetic compounds of the hydrophobic ZZxxZ and ZxxZZ sequences (Z = Leu or Phe) inhibited HIF transcriptional activity and/or anti-rabies viral activity, revealing that our designed diazatricyclododecene 3D-scaffold **8a** has potential to be a versatile peptide mimic skeleton. We believe that peptide mimicry based on rigid 3D scaffolds can provide a new perspective for generating bioactive compounds. Further development of novel 3D scaffolds and bioactive compounds based on these scaffolds is currently being conducted in our laboratory.

Acknowledgements

We thank Mr Yoshihisa Sei (Open Facility Center, Materials Analysis Division Tokyo Institute of Technology) for his technical support with X-ray crystallographic analysis.

Conflict of interest

The authors declare no conflict of interest.

Keywords: 3D scaffold • chemical space • gold catalysis • peptidomimetic • pharmacophore fitting

[1] S. R. Langdon, N. Brown, J. Blagg, *J. Chem. Inf. Model.* **2011**, *51*, 2174-2185.

[2] D. G. Brown, J. Boström, *J. Med. Chem.* **2016**, *59*, 4443–4458.

[3] a) S. Dandapani, L. A. Marcaurelle, *Nat. Chem. Biol.* **2010**, *6*, 861-863; b) A. Barker, J. G. Kettle, T. Nowak, J. E. Pease, *Drug Discov. Today* **2013**, *18*, 298-304; c) M. R. Arkin, J. A. Wells, *Nat Rev Drug Discov* **2004**, *3*, 301–317.

[4] a) S. L. Schreiber, *Science* **2000**, *287*, 1964-1969; b) W. R. J. D. Galloway, A. Isidro-Llobet, D. R. Spring, *Nat. Commun.* **2010**, *1*, 1-13; c) C. J. Gerry, S. L. Schreiber, *Curr. Opin. Chem. Biol.* **2020**, *56*, 1-9.

[5] a) S. Wetzel, R. S. Bon, K. Kumar, H. Waldmann, *Angew. Chem. Int. Ed.* **2011**, *50*, 10800-10826; *Angew. Chem.* **2011**, *123*, 10990-11018; b) H. van Hattum, H. Waldmann, *J. Am. Chem. Soc.* **2014**, *136*, 11853–11859.

[6] J. Kim, J. Jung, J. Koo, W. Cho, W. S. Lee, C. Kim, W. Park, S. B. Park, *Nat. Commun.* **2016**, *7*, 13196.

[7] P. Y. Ng, Y. Tang, W. M. Knosp, H. S. Stadler, J. T. Shaw, *Angew. Chem. Int. Ed.* **2007**, *46*, 5352-5355; *Angew. Chem.* **2007**, *119*, 5448-5451.

[8] G. Karageorgis, D. J. Foley, L. Laraia, H. Waldmann, *Nat. Chem.* **2020**, *12*, 227-235.

[9] D. J. Foley, S. Zinken, D. Corkery, L. Laraia, A. Pahl, Y.-W. Wu, H. Waldmann, *Angew, Chem, Int, Ed.* **2020**, *59*, 12470-12476; *Angew. Chem.* **2020**, *132*, 12570-12576.

[10] F. M. Tajabadi, R. H. Pouwer, M. Liu, Y. Dashti, M. R. Campitelli, M. Murtaza, G. D. Mellick, S. A. Wood, I. D. Jenkins, R. J. Quinn, *J. Med. Chem.* **2018**, *61*, 6609−6628.

[11] a) A. J. Souers, J. D. Leverson, E. R. Boghaert, S. L. Ackler, N. D. Catron, J. Chen, B. D. Dayton, H. Ding, S. H. Enschede, W. J. Fairbrother, D. C. S. Huang, S. G. Hymowitz, S. Jin, S. L. Khaw, P. J. Kovar, L. T. Lam, J. Lee, H. L. Maecker, K. C. Marsh, K. D. Mason, M. J. Mitten, P. M. Nimmer, A. Oleksijew, C. H. Park, C.-M. Park, D. C. Phillips, A. W. Roberts, D. Sampath, J. F. Seymour, M. L. Smith, G. M. Sullivan, S. K. Tahir, C. Tse, M. D. Wendt, Y. Xiao, J. C. Xue, H. Zhang, R. A. Humerickhouse, S. H. Rosenberg, S. W. Elmore, *Nat. Med.* **2013**, *19*, 202−208; b) C. M. Croce, J. C. Reed, *Cancer Res.* **2016**, *76*, 5914−5920; c) H. Lu, Q. Zhou, J. He, Z. Jiang, C. Peng, R. Tong, J. Shi, *Signal Transduct. Target. Ther.* **2020**, *5*, 213.

[12] a) A. M. Petros, J. Dinges, D. J. Augeri, S. A. Baumeister, D. A. Betebenner, M. G. Bures, S. W. Elmore, P. J. Hajduk, M. K. Joseph, S. K. Landis, D. G. Nettesheim, S. H. Rosenberg, W. Shen, S. Thomas, X. Wang, I. Zanze, H. Zhang, S. W. Fesik, *J. Med. Chem.* **2006**, *49*, 656−663; b) C. Tse, A. R. Shoemaker, J. Adickes, M. G. Anderson, J. Chen, S. Jin, E. F. Johnson, K. C. Marsh, M. J. Mitten, P. Nimmer, L. Roberts, S. K. Tahir, Y. Xiao, X. Yang, H. Zhang, S. Fesik, S. H. Rosenberg, S. W. Elmore, *Cancer Res.* **2008**, *68*, 3421−3428.

[13] a) M. Pelay-Gimeno, A. Glas, O. Koch, T. N. Grossmann, *Angew. Chem. Int. Ed.* **2015**, *54*, 8896-8927; *Angew. Chem.* **2015**, *127*, 9022-9054; b) C. Sheng, G. Dong, Z. Miao, W. Zhang, W. Wang. *Chem. Soc. Rev*, **2015**, *44*, 8238-8259; c) L. Mabonga, A. P. Kappo, *Int. J. Pept. Res. Therapeut.* **2020**, *26*, 225–241.

[14] W. P. Nolan, G. S. Ratcliffe, D. C. Rees, *Tetrahedron Lett.* **1992**, *33*, 6879-6882.

[15] B. P. Orner, J. T. Ernst, A. D. Hamilton, *J. Am. Chem. Soc.* **2001**, *123*, 5382-5383.

[16] J.-M. Ahn, S.-Y. Han, *Tetrahedron Lett.* **2007**, *48*, 3543-3547.

[17] A. Volonterio, L. Moisan, J. Rebek, *Org. Lett.* **2007**, *9*, 3733-3736.

[18] J. H. Lee, Q. Zhang, S. Jo, S. C. Chai, M. Oh, W. Im, H. Lu, H.-S. Lim, *J. Am. Chem. Soc.* **2011**, *133*, 676-679.

[19] P. Tošoská, P. S. Arora, *Org. Lett.* **2010**, *12*, 1588-1591.

[20] B. B. Lao, I. Grishagin, H. Mesallati, T. F. Brewer, B. Z. Olenyuk, P. S. Arora. *Proc. Natl. Acad. Sci. USA* **2014**, *111*, 7531–7536.

[21] H. Ueda, A. Yoshimori, H. Nakamura, *Bioorg. Med. Chem.* **2018**, *26*, 3345-3351.

[22] V. D. Pont, R. K. Plemper, M. J. Schnell, *Curr. Opin. Virol.* **2019**, *35*, 1-13.

[23] A. A. V. Albertini, A. K. Wernimont, T. Muziol, R. B. G. Ravelli, C. R. Clapier, G. Schoehn, W. Weissenhorn, R. W. H. Ruigrok, *Science*, **2006**, *313*, 360-363.

[24] a) S. T. Staben, J. J. Kennedy-Smith, D. Huang, B. K. Corkey, R. L. LaLonde, F. D. Toste, *Angew. Chem. Int. Ed.* **2006**, *45*, 5991-5994; *Angew. Chem.* **2006**, *118*, 6137-6140; b) F. Barabé, G. Bétournay, G. Bellavance, L. Barriault, *Org. Lett.* **2009**, *11*, 4236-4238; c) A. Carrër, C. Péan, F. Perron-Sierra, O. Mirguet, V. Michelet, *Adv. Synth.* Catal. **2016**, *358*, 1540-1545.

10.1002/chem.202101440

[25] R. H. Mach, R. R. Luedtke, C. D. Unsworth, V. A. Boundy, P. A. Nowak, J. G. Scripko, S. T. Elder, J. R. Jackson, P. L. Hoffmann, P. H. Evora, A. V. Rao, P. B. Molinoff, S. R. Childers, R. L. Ehrenkaufer, *J. Med. Chem*. **1993**, *36*, 3707-3720.
[26] M. B. Lauber, S. S. Stahl, *ACS Catal*. **2013**, *3*, 2612-2616.
[27] P. Chen, H, Yang, H. Zhang, W. Chen, Z. Zhang, J. Zhang, H. Li, X. Wang, X. Xie, X. She, *Org. Lett*. **2020**, *22*, 2022-2025.
[28] Y. Fricke, N. Kopp, B. Wünsch, *Synthesis* **2010**, 791-796.
[29] E. M. F. Billaud, L. Rbah-Vidal, A. Vidal, S. Besse, S. Tarrit, S. Askienazy, A. Maisonial, N. Moins, J.-C. Madelmont, E. Miot-Noirault, J.-M. Chezal, P. Auzeloux. *J. Med. Chem.* **2013**, *56*, 8455-8467.
[30] G. Wolber, T. Langer, *J. Chem. Inf. Model.* **2005**, *45*, 160–169.
[31] W. H. B. Sauer, M. K. Schwarz, *J. Chem. Inf. Comput. Sci*. **2003**, *43*, 987-1003.
[32] E.-J. Yeo, Y.-S. Chun, Y.-S. Cho, J. Kim, J.-C. Lee, M.-S. Kim, J.-W. Park, *J. Natl. Cancer Inst.* **2003**, *95*, 516-525.
[33] K. Yamada, K. Noguchi, T. Komeno, Y. Furuta, A. Nishizono, *J. Infect. Dis*. **2016**, *213*, 1253-1261.

10.1002/chem.202101440

Entry for the Table of Contents

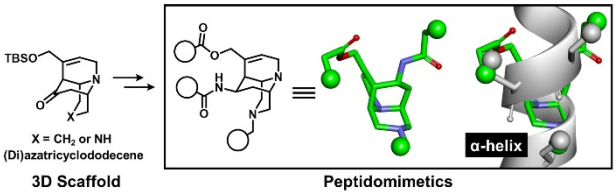

Three-dimensional (3D) scaffolds have the potential to provide unique bioactivity, which cannot be achieved by conventional flat aromatic ring- based compounds. (Di)azatricyclododecene scaffold with a bridged tricyclic system was developed and applied to design peptidomimetics with a 3D scaffold. The designed peptidomimetics showed inhibition of HIF transcription activity and antiviral activity toward rabies virus, both of which α-helix peptide mediated interaction play a pivotal role.